

Aluminium surface modification by nitrogen-argon mixture PIII

H. Millán-Flores, R. López-Callejas^{1,2,*}, E. E. Granda-Gutiérrez, A. de la Piedad-Benítez

¹*Instituto Tecnológico de Toluca
AP 890, Toluca, Estado de México, México*

A. E. Muñoz-Castro, R. Valencia A., R. Peña-Eguiluz, A. Mercado-Cabrera, S. R. Barocio

²*Instituto Nacional de Investigaciones Nucleares
AP 18-1027, 11801 México DF*

(Recibido: 5 de marzo de 2009; Aceptado: 29 de mayo de 2009)

Pure nitrogen, 30% argon/70% nitrogen, 50% argon/50% nitrogen, 70% argon/30% nitrogen plasma immersion ion implantation (PIII) processes onto aluminium samples has been performed at 2 to 6 kV negative bias and 50 to 150 μ s pulse widths, the sample temperature being established at 400 °C. Incident fluencies of $\sim 10^{18}$ atoms/cm² were used to investigate the diffusion behaviour and AlN phase formation in the samples. X-ray diffraction (XRD) shows the formation of the cubic phase of AlN with both pure nitrogen and all the mixtures whereas the hexagonal phase becomes apparent only in the 50% mixture and in pure nitrogen. The characteristic peak of AlN has also been determined by Raman spectroscopy. The microhardness was found to be always maximal with the 50% nitrogen 50% argon mixture.

Keywords: plasma immersion ion implantation, X-ray diffraction, hardness, scanning electron microscopy, surface modification

1. Introduction

Aluminium and its alloys are attractive materials to the car, aviation, food and chemical industries as much as to the pharmaceutical technology. However, these materials lack surface hardness and other tribological qualities which limit their applications.. Nitriding is an effective surface modification process used to enhance corrosion resistance in addition to improving wear resistance due to the resulting high hardness of the nitrided surface. The formation of aluminium nitride (AlN) during nitrogen ion implantation on pure aluminium has been investigated extensively in conventional beam line implantation [1] and now in plasma (source) ion implantation (PSII or PIII) on pure aluminium and its alloys [2]-[4].

In this paper we report on the feasibility of forming an AlN layer at low energy by a plasma immersion ion implantation (PIII) process onto aluminium samples at incident fluencies of $\sim 10^{18}$ atoms/cm². The PIII process has been carried out in both pure nitrogen and different argon/nitrogen mixtures.

2. Experimental set-up

An aluminium rod was cut in cylindrical pieces, 10 mm in diameter and with a 5 mm thickness. The samples were mirror polished and ultrasonically cleansed in acetone. Then, they were introduced into the SS-304 stainless process chamber with cylindrical geometry, 0.6 m long and 0.3 m in diameter. A base pressure of 10^{-6} Torr ($\sim 10^{-4}$ Pa) was achieved with a turbomolecular vacuum pump, and then the gas pressure was established at 2×10^{-2} Torr (~ 2.66 Pa) by admitting the selected implantation gas. Each

sample receives a previous 30 minute cleansing stay in an argon plasma to be finally implanted during 3.5-4.5 hour periods with 70%N-30%Ar, 50%N-50%Ar, 70%N-30%Ar and nitrogen (99.995% pure) plasmas.

The plasma discharge has been produced using a constant current DC power supply with a maximum output power of 1200W. This supply has been specifically designed and constructed, based on a current-source converter (CSC) operating in a resonant mode [5]. The discharge was established at a constant 2000 mA current leading to an electron plasma density of about 5×10^{16} m⁻³, which was measured with a 0.98 mm long 0.34 mm diameter double cylindrical probe [6]. After that, the samples were biased by means of a high voltage pulse modulator (HVM) driven at a 50-150 μ s pulse width with a repetition rate of 0.5-2 kHz and 1-6 kV in amplitude.

With an aim to evaluate the efficiency of the PIII process in the treatment of aluminium, different techniques of superficial analysis were used including: profilometry, Vickers microhardness tests, x-ray diffractometry, scanning electron microscopy and Raman spectroscopy.

3. Results and discussion

3.1. 400°C/150μs/2kV samples

The implantation bias being maintained at 2kV with a 150 μ s pulse width, a 400 °C sample temperature was established. The resulting aluminium morphology is shown in the micrographs of Fig. 1. In spite of the apparent surface roughness of the pure nitrogen plasma treated samples (Fig. 1.a) their profilometric measurement yields

*e -mail: regulo.lopez@inin.gob.mx

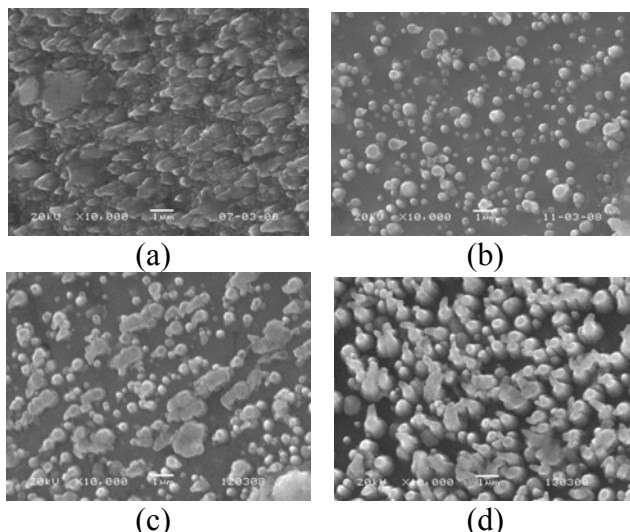


Figure 1. Micrographs of samples treated at 400°C/150μs/2kV: a) Ar(N), b) Ar/(N70-Ar30), c) Ar/(N50-Ar50), d) Ar/(N30-Ar70).

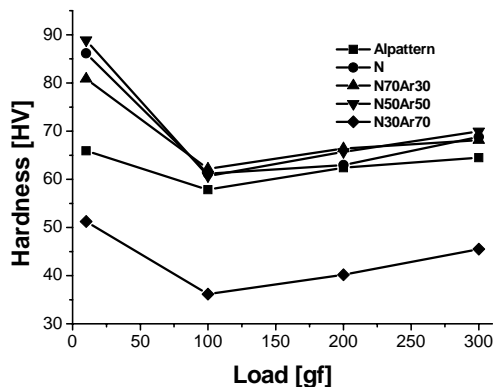


Figure 2. Microhardness at 400°C/150μs/2kV

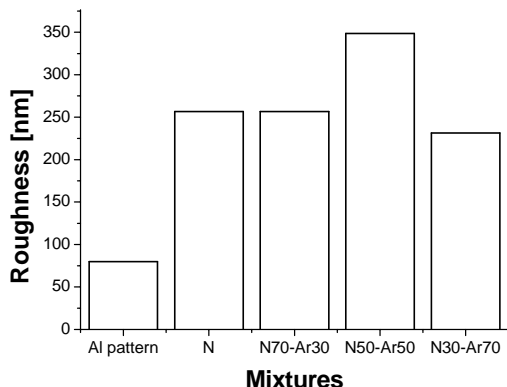


Figure 3. Roughness at 400°C/150μs/2kV.

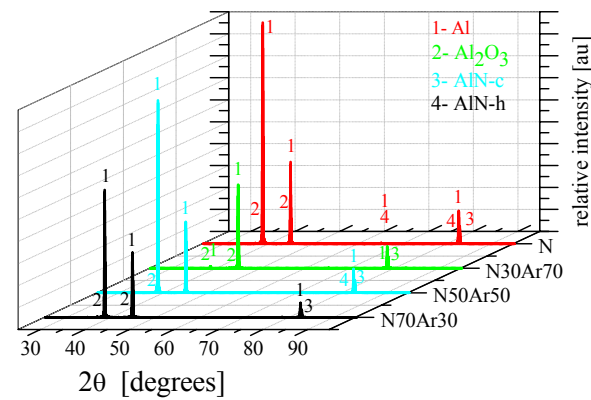


Figure 4. Diffractograms at 400°C/150μs/2kV samples.

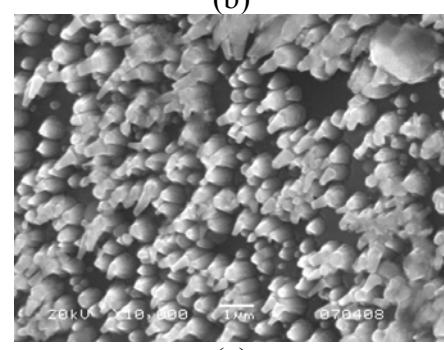
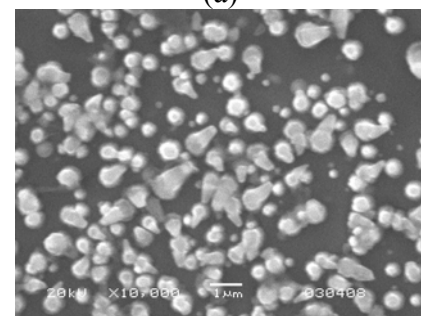
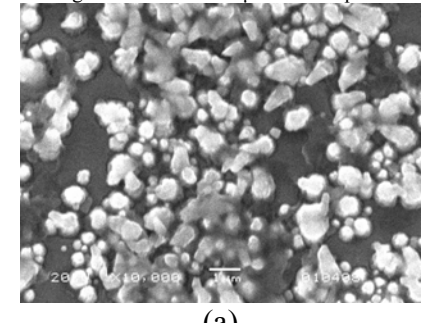


Figure 5. Micrographs of the 400°C/150μs/2kV samples: a) N70%-Ar30%, b) N50%-Ar50%, c) N30%-Ar70%.

similar values to those of the samples in Figs. 1.b and 1.c, as confirmed by Fig. 2. By contrast, the N50%-Ar50% plasma treated sample, seen in Fig. 1.c, presents a much more pronounced roughness attributable to its larger rather flat more clustered excrescences.

The outcome of the microhardness tests can be seen in Fig. 3. It seems remarkable that the N30%-Ar70% treated samples exhibit even lower values than that of the untreated control one; in all other cases the microhardness increased. There appears to exist a correlation between the microhardness and the nitrogen concentration increases (Fig. 3) whereby the N, N70%-Ar30% and N50%-Ar50% implanted samples achieved 61HV0.1, 62HV0.1 and 61HV.01 respectively: a correlation not observed in the N30%-Ar70% treated samples. It would then follow the convenience of implanting in an equal part mixture plasma with the additional bonus of a roughness not inferior to ~350nm (Fig. 2).

Fig. 4 displays the x ray diffractogrammes of samples treated in plasmas of several compositions. A maximal content of the AlN in its cubic and hexagonal phases is found in the pure nitrogen case (Fig. 4.a). The peak found at $2\theta = 65.13^\circ$, which can be associated to Al according to the 4-0787 JCPDS file Standard, also outstands in the pure N plasma lot, albeit it is also present with a low intensity in the N70%-Ar30% and N30%-Ar70% samples (Figs. 4.b and 4.d). Even lower amplitudes are attained with N30%-Ar70% and barely perceptible with N50%-Ar50%.

The diffractogramme in Fig. 4.b points to a high concentration of Al_2O_3 as well as the cubic phase of AlN; Fig. 4.c reveals a greater cubic AlN concentration along with more intense Al_2O_3 peaks. Fig. 4.d corresponds to an instance of the N30%-Ar70% treatment with two low intensity Al_2O_3 peaks (4-0787 JCPDS) along with an amplified one at $2\theta = 78.23^\circ$ and another, depressed, at $2\theta = 82.43^\circ$ suggesting some deformation of the material. Thus, an increasing deformation of the samples could be inferred from equally increasing Ar concentrations while greater N concentrations would lead to more AlN abundance.

3.2. $400^\circ\text{C}/75\mu\text{s}/3.5\text{kV}$ samples

Once the samples of this lot were biased at 3.5 kV so to keep them at a 400° its implantation took place with $75\ \mu\text{s}$ long pulses in order to increase the energy of the oncoming ions. The resulting micrographs are shown in Fig. 5 where the more visually pronounced roughness is achieved with the N30%-Ar70% mixture (Fig. 5.c) although, numerically speaking, the roughest one turns out to be the N50%-Ar50%, as validated by the profilometry tests (Fig.6). The morphological differences between the N30%-Ar70% and the control samples are quite evident.

As seen in the microhardness plot (Fig. 7), under a 100 g load, the best hardened sample turned out to be the one with the highest N content, ie N70%-Ar30%, reaching 62HV0.1 while the N30%-Ar70% one only accounted for

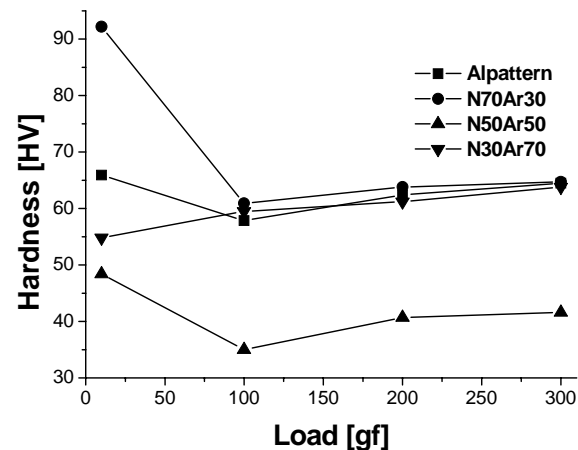


Figure 6. Microhardness at $400^\circ\text{C}/75\mu\text{s}/2\text{kV}$.

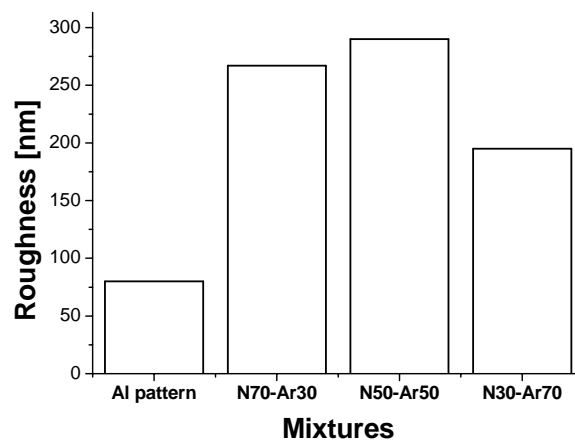


Figure 7. Roughness at $400^\circ\text{C}/75\mu\text{s}/2\text{kV}$.

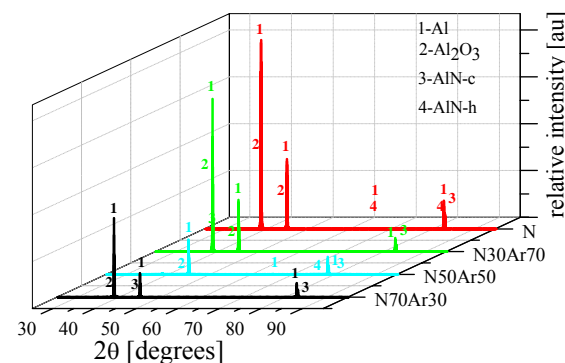


Figure 8. Diffractograms at $400^\circ\text{C}/75\mu\text{s}/3.5\text{kV}$ samples.

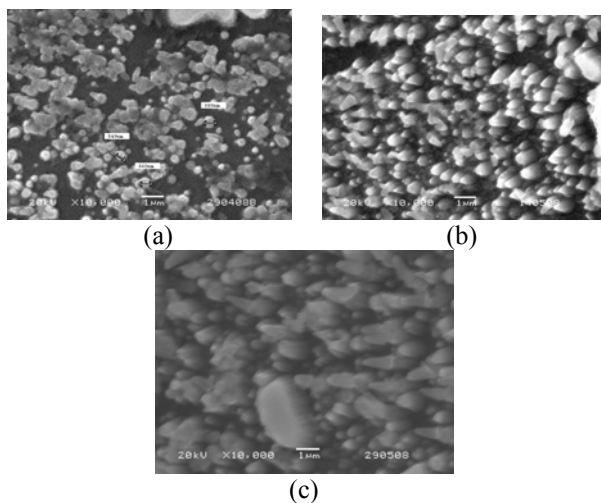


Figure 9. 400°C/50μs/6kV sample micrographs: a) N50%-Ar50% 4.5h, b) pure N 4.5hr, c) pure N 3.5h.

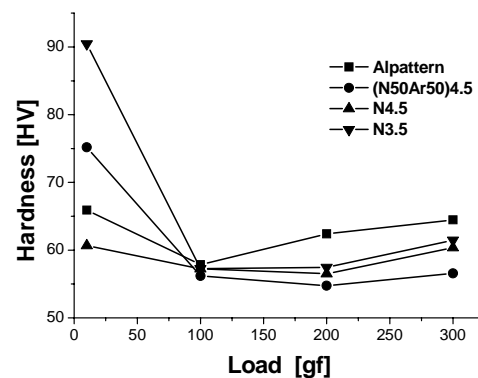


Figure 10. Microhardness of the 400°C/50μs/6kV samples.

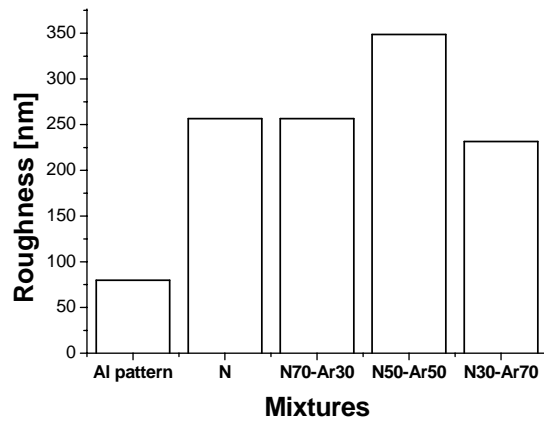


Figure 11. Roughness of the 400°C/50μs/6kV samples.

60HV0.1, in both cases greater than the control sample microhardness. The smallest 35HV0.1 value corresponded to the equal part mixture samples.

Fig. 6 indicates that N50%-Ar50% samples present the highest degree of roughness and yet the poorest microhardness (Fig. 7). Likewise, the N70%-Ar30% sample barely reaches the average roughness value 267 nm despite its large N content, which would have implied a greater roughness resulting from a larger ion population. On its part, the N30%-Ar70% sample yielded 195 nm: the lowest value of the 75 μs pulse width lot.

The x-ray diffractograms from the 400°C/75μs/3.5kV samples can be seen in Fig. 8. The relative intensity of the Al peak at $2\theta = 38.47^\circ$ is smaller in the N50%-Ar50% case than in the N70%-Ar30% and N30%-Ar70% ones (Figs. 8.a, 8.b). A different situation happens to the $2\theta = 78.23^\circ$ peak (Fig. 8.b) greater than those in Figs. 8.a and 8.c, which could be interpreted as a poor concentration of AlN and compounds alike leading to diminished peak amplitudes, on top of the inherently small main Al peaks, taking those like the one at $2\theta = 65.13^\circ$ to the complete extinction. The N50%-Ar50% diffractogram in Fig. 8.b exhibits a very depressed main Al peak and does not show the $2\theta = 82.43^\circ$ Al peak as a possible result from the structure change created by the implantation process. Meanwhile, Fig. 8.c suggests that a low N concentration is conducive to the formation of the AlN cubic phase at the 2θ angles: 41.80° (87-1053 JCPDS file), 78.41° and 82.62° (46-1200 JCPDS file).

3.3 400°C/50μs/6kV samples

The morphological alterations of the samples treated in the 50 μs 6 kV region, include a maximal roughness in the pure N 4.5 hour treated ones (Fig. 9.b). By comparison, the N50%-Ar50% 4.5 hour sample in Fig. 9.a exhibits flat deposits on the surface in the order of 565 nm. Then, a pure N 3.5 hour case in Fig. 9.c presents a noticeably irregular surface although the sample roughness is not the highest.

As follows from Fig. 10, the maximal roughness in the lot is achieved by the pure N longest implantation. The lowest value is also the result of pure N but with a 3.5 hour processing. Meanwhile, the remarkable microhardness outcome in Fig. 11 indicates that, at loads greater than 100 g, all the treated samples in the lot lose some of their hardness with respect to that of the control sample, instead of increasing them.

Representative samples of the lot were transversally cut and mirror polished in order to analyse the implanted layer depth. Fig. 12 shows that the N50%-Ar50% treatment produces a ~300 nm thick layer with three different morphologies which proved to contain a high N concentration. The pure N 4.5 hour (Fig. 12.b) and pure N 3.5 hour (Fig. 12.c) cases presented two morphologies only, the former having produced a ~500 nm layer similarly rich in N. The pure N 4.5 hour sample, by

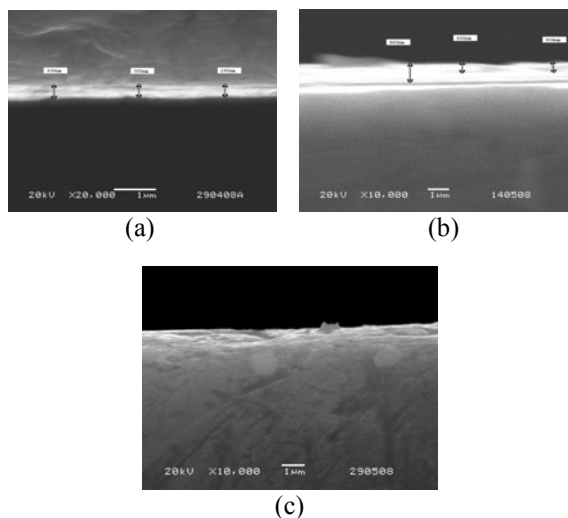


Figure 12. Cross section micrographs of the 400°C/150μs/2kV sample lot: a) N50%-Ar50% 4.5h, b) pure N 4.5hr, c) pure N 3.5h

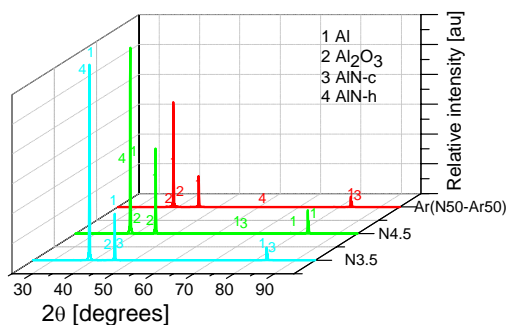


Figure 13. 400°C/50μs/6kV surface diffractograms: a) N50%-Ar50% 4.5h, b) pure N 4.5hr, c) pure N 3.5h.

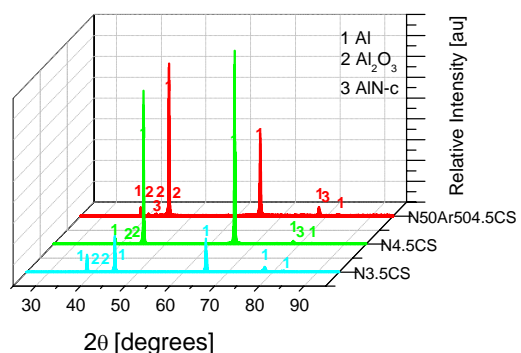


Figure 14. 400°C/50μs/6kV cross section diffractograms: a) N50%-Ar50% 4.5h, b) pure N 4.5hr, c) pure N 3.5h.

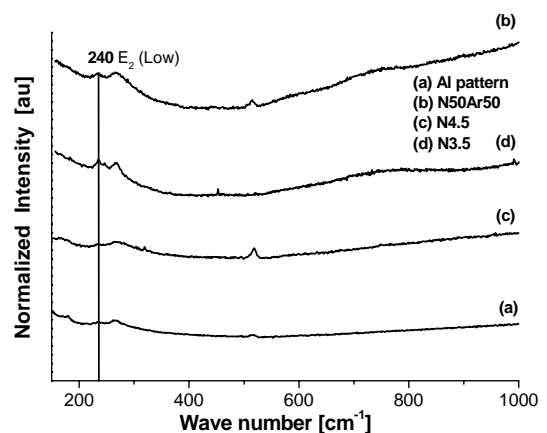


Figure 15. 400°C/50μs/6kV Raman spectra.

contrast, displayed a layer thin beyond the equipment resolution as well as a very poor N content.

The diffractograms of the sample lot detect the presence of AlN in both its cubic (c) and hexagonal (h) phases. The N50%-Ar50% 4.5h pattern (Fig. 13. a) contains all the peaks of Al although with a diminished relative intensity at $2\theta = 78.23^\circ$ and an enhanced one at $2\theta = 82.43^\circ$, with respect to the 4-0787 JCPDS file standard which points to some distortion in the substrate. The presence of Al₂O₃ is hinted by low intensity peaks that can be attributed to the sudden oxidation of the sample when it is taken out of the implantation chamber. AlN is mostly present in its cubic form with only one visible AlN-h peak. The peak at $2\theta = 82.43^\circ$ is considerable higher in the pure N 4.5 h sample (Fig. 13.b) than in the N50%-Ar50% 4.5 h, pure N 3.5 h (Figs. 13.a and 13.c, respectively). The proportion between the hexagonal and cubic phases remains practically unchanged; yet, the oxygen content is higher as shown by the amplified Al₂O₃ peaks. The cubic AlN peaks are more numerous in the pure N 3.5h pattern (Fig. 13.c) although only one of the hexagonal phase. The Al peak at $2\theta = 82.43^\circ$ retains its high intensity.

The cross section diffractograms shown in Fig. 14 portray a low presence of AlN in either phase in spite of the occurrence of the characteristic N peaks. The N50%-Ar50% 4.5h and pure N 4.5hr patterns in particular (Figs. 14.a and 14.b) detect the existence of AlN, contrary to the outcome of the pure N 3.5h case (Fig. 14.c). Nevertheless the Al₂O₃ peaks remain in position at $2\theta = 40.22^\circ$, 41.98° (12-0539 JCPDS file) and 42.76° (24-0493 JCPDS file).

The Raman analysis of the control and treated samples of the lot was carried out with a Si calibrated 633 nm He-Ne laser capable of 10 data acquisitions per minute, covering a 150-1000 cm⁻¹ wave number range. The results at 240 cm⁻¹, characteristic of AlN, are displayed in Fig. 15. As expected, the response of the untreated Al sample pattern at this wave length differs from the rest. Of them, the pure N 3.5h peak is more pronounced than that of the N50%-Ar50% 4.5h sample, the pure N 4.5 h response being the weakest, although still perceptible. The intensity of the

control sample and that of the N50%-Ar50% 4.5 h one turned to be the lowest and highest, respectively. The 514 cm⁻¹ peak in Fig. 15, also typical of AlN, is visible in the N50%-Ar50% 4.5 h and pure N 4.5 h spectra as well as in that of pure N 3.5 h, albeit with some leftward shift.

Conclusions

Aluminium has been PIII implanted with either pure nitrogen or argon/nitrogen mixtures at a 400°C sample temperature using incident fluencies of $\sim 10^{18}$ atoms/cm² during 3.5-4.5 hour periods. The maximal microhardness values were found in samples treated with the equal part mixture and biased between 2 kV and 6 kV. The maximal roughness was achieved with this gas mixture in all cases, although increasing along with the implantation pulse width up to a 350 nm peak at 150 μ s. The latter critical value remains invariant under the pure nitrogen plasma, provided that longer 4.5 hour implantation periods are carried out.

X ray diffraction studies have validated the formation of the cubic phase of AlN at a 41.806° angle, given the 87-1053 JCPDS file Standard, in samples treated with both the gas mixtures and pure nitrogen. Likewise, the presence of the hexagonal phase has been detected when either pure nitrogen or the 50% mixture have been used. The signature

peak of AlN has also been confirmed by Raman spectroscopy.

Acknowledgements

This work received financial support from CONACYT and DGEST, Mexico. The authors are grateful to the technical collaboration received from M. T. Torres M., I. Contreras V. and P. Angeles E.

References

- [1]. M. Ueda, H. Reuther and C.M. Lepienski, Nucl. Instrum. and Meth. in Phys. Research Section B, **240**, 199 (2005).
- [2]. D. Manova, P. Huber, S. Mändl, B. Rauschenbach, Surf. And Coat. Technol. **128-129**, 249 (2000).
- [3]. X. L. Xiao, D. G. McCulloch D. R. McKenzie and M. M. M. Bilek, J. of Appl. Phys., **100-1**, 013504 (2006).
- [4]. E. Valcheva, S. Dimitrov, D. Manova, S. Mändl and S. Alexandrova, Surf. and Coat. Technol., **202-11**, 2319 (2008).
- [5]. E. E. Granda-Gutiérrez, R. López-Callejas, R. Peña-Eguiluz, A. Mercado-Cabrera, R. Valencia A., S. R. Barocio, O. G. Godoy-Cabrera, A. de la Piedad-Beneitez, J. S. Benitez-Read and J. O. Pacheco-Sotelo; Proc. 25th IASTED Int. Conf. on Modelling, Identification and Control, **500**, 255 (2006).
- [6]. R. López-Callejas, R. Valencia-Alvarado, A. E. Muñoz-Castro, J. L. Tapia-Fabela, Rev. Sci. Instrum., **73**, 4277 (2002).